CrystEngComm

RSC Publishing

COMMUNICATION

Additive-mediated size control of MOF nanoparticles†

Annekathrin Ranft,[ab] Sophia B. Betzler,[b] Frederik Haase[ab] and Bettina V. Lotsch*[ab]

A fast synthesis approach toward sub-60 nm sized MOF nanoparticles was developed by employing auxiliary additives. Control over the size of HKUST-1 and IRMOF-3 particles was gained by adjusting the concentration and type of stabilizers. Colloidal solutions of the MOFs were used for the formation of optically homogeneous thin films by spin-coating.

Metal–organic frameworks (MOFs) represent a class of crystalline porous materials featuring intriguing properties such as chemical functionality combined with high porosity, which can be tailored for desired applications through the choice of the constituting building blocks.[1] Possible fields of application range from gas adsorption and storage[2] over catalysis[3] and molecular sieving[4] to the use of MOFs as active components in chemical sensors.[5] Especially in the field of sensing, the possibility to cast the sensing material into a suitable form, such as thin films, is a key prerequisite to ensure diffusion throughout the entire active material and to keep response times low.[6] MOF nanoparticles (NPs) can serve as versatile building blocks for thin films, which can be obtained by straightforward, low temperature solution processing protocols such as spin- and dip-coating.[7] At the same time, the use of nanoparticulate MOFs in principle allows for the precise adjustment of the material's properties, such as surface chemistry and shape, which in turn will affect the microstructure and, hence, performance of the resulting MOF film; besides, shape-specific synthesis strategies could reveal a better insight into MOF crystal growth mechanisms at the nanoscale.[8]

Among a range of well-studied MOF systems, HKUST-1 ($Cu_3(BTC)_2$, BTC = benzene-1,3,5-tricarboxylate) belongs to the most prominent ones owing to its structural stability on ad- and desorption of water molecules, which coordinate to unsaturated Cu(ıı) sites of the framework.[9] In addition, such open metal sites are proposed to show increased affinity towards H_2 molecules resulting in improved hydrogen storage capacity,[10] which may be even enhanced by tailoring the morphology and size of HKUST-1 crystals on the nanoscale. Access to MOF NPs has been obtained by a number of methods so far, upon which ultrasonic (US) or microwave (MW) assisted heating have been found to significantly accelerate the crystallization of MOFs as compared to traditional electric heating.[11–13] However, these strategies have shown to lack reproducibility owing to the use of different types of synthesis set-ups which may affect the particle properties significantly.[14] The need for high temperatures for enhanced crystallinity has been circumvented by the development of direct mixing approaches,[12,15–17] mechanochemical routes,[18] freeze–drying approaches[19] or continuous-flow methods which allow for the high-throughput preparation of MOF crystals by rapid mixing of pre-heated solvent streams.[20] Such routes suffer, however, in some cases from comparatively long reaction times (20 min at least for the synthesis of HKUST-1 based on a mechanochemical route[18]) or a complex synthesis set-up (synthesis in a continuous flow reactor[20]) which hampers their generalization and implementation. Moreover, fine-tuning of the crystal size below 100 nm remains a challenge for the above mentioned synthesis strategies. Another attractive route to the size-controlled MOF synthesis is the use of auxiliary additives which can act as competitors to the bridging ligand ("coordination modulation"),[13,21,22] or the use of surfactants to control the influx of monomers in order to stabilize the growing particles and to control the particles' morphology through weak interactions of the additive with the particle surface ("surfactant-mediated synthesis").[23–26] These synthesis schemes have been successfully utilized not only for

a Max Planck Institute for Solid State Research, Heisenbergstr. 1, 70569 Stuttgart, Germany. E-mail: b.lotsch@fkf.mpg.de; Fax: +49 711689-1612; Tel: +49 711689-1610
b Department of Chemistry, University of Munich (LMU), Butenandtstr. 5-13, 81377 Munich, Germany. E-mail: bettina.lotsch@cup.uni-muenchen.de; Fax: +49 892180-77806; Tel: +49 892180-77429

HKUST-1 with the help of PAA (poly(acrylic acid)) salts[25] or dodecanoic acid as size modulating agents,[13] but also for other well-studied MOFs such as isoreticular IRMOF-3 ($Zn_4O(BDC–NH_2)_3$, $BDC–NH_2$ = 2-aminoterephthalate). In the case of IRMOF-3, superior control of the crystal size has been achieved by the addition of CTAB (hexadecyltrimethylammonium bromide) to slow down nucleation times, and by fine-tuning the synthesis conditions through a four-step strategy.[26] Based on these studies realizing the size-controlled formation of MOFs at ambient rather than high-temperature conditions,[27–29] the controlled synthesis of nanosized MOFs seems feasible. Nevertheless, only a few generally applicable synthetic strategies toward nanoMOFs with sizes less than 100 nm have been developed as yet.

In this study, we report on the preparation of ultrasmall versions of HKUST-1 and IRMOF-3, using an additive-mediated synthesis strategy. Our approach involves the use of chemical additives (polymers or polymer–surfactant combinations), which are mixed with the ligand before being reacted with the respective metal source, upon which MOF NPs form within 5 minutes under mild conditions. By altering the synthetic conditions such as reaction temperature, concentration, ratio and type of additive, we gain control over the particle size of the respective MOF.

HKUST-1 NPs were successfully prepared by mixing precursor solutions ($Cu(OAc)_2 \cdot H_2O$ and trimesic acid (H_3BTC) in a water–ethanol–DMF mixture) with PAA at different temperatures (0 °C, room temperature (RT), 55 °C). Powder X-ray diffraction (PXRD) patterns of the products obtained at 0 °C and at RT, respectively, confirm the structure of the as-synthesized materials (Fig. 1a), apart from peak broadening, which is attributed to the small grain size of the products (29 nm deduced through the Scherrer formula).

The morphology of the MOF NPs was examined by scanning electron microscopy (SEM), atomic force microscopy (AFM) and dynamic light scattering (DLS). SEM images of HKUST-1 synthesized at RT and 0 °C, respectively, reveal small particles with diameters between 30 nm and 50 nm (Fig. 2a), which was confirmed additionally through AFM (see Fig. 2b and S1, ESI†). DLS measurements (Fig. S2, ESI†) suggest that an increase of the reaction temperature from 0 °C to RT leads to a small shift of the mean particle radius from 50 nm to 60 nm (note that DLS measures the hydrodynamic
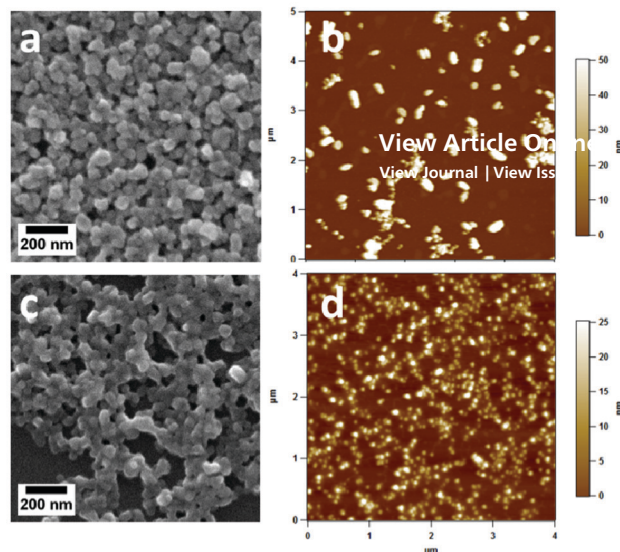

Fig. 2 SEM and AFM images of HKUST-1 and IRMOF-3 particles. (a) SEM image of HKUST-1 synthesized at RT, (b) AFM image of HKUST-1 synthesized at 0 °C, (c) SEM image and (d) AFM image of IRMOF-3 synthesized with a ratio of CTAB/PVP = 0.027 mmol/0.00025 mmol.

radius including a solvating shell, leading to larger particle sizes than obtained by direct imaging techniques). This observation is supported by SEM images showing a comparatively larger amount of particles with diameters >40 nm for the synthesis at RT (see Fig. S3, ESI†). Heating the reaction mixture to 55 °C, however, leads to a more significant increase of the particle radius from 60 nm to 80 nm, as confirmed by DLS measurements (Fig. S2, ESI†). Low temperatures, therefore, seem to be beneficial to slow down crystal growth and reduce the particle size of HKUST-1; this tendency is in agreement with other reports where size-control was gained by using rather mild synthesis conditions.[16] We observed a similar size-controlling effect by varying the polymer concentration, i.e. the ratio of H_3BTC to PAA, from 1:2 up to 1:15 (corresponding to 0.082 mmol up to 0.615 mmol of PAA), while keeping the temperature at 0 °C and monitoring the change of the particle size with DLS (Fig. S4, ESI†). We observe that on decreasing the amount of PAA, the particle radius decreases from 57 nm (for a ratio of 1:6, 0.246 mmol PAA) to 48 nm (for a ratio of 1:3, 0.123 mmol PAA) while the size distribution is significantly narrowed as indicated by a change of the polydispersity index (PdI) from 0.184 (1:6, 0.246 mmol PAA) to 0.091 (1:3, 0.123 mmol PAA). However, for an even lower ratio of 1:2 (0.082 mmol PAA), the PdI was found to rise again (0.176). While the size distribution is broadened – in general – with increasing amounts of PAA, the product yield is decreased, and at the highest PAA concentration (1:15, 0.615 mmol PAA) no precipitation was observed at all. We rationalize these findings by invoking the observation that HKUST-1 is formed within seconds upon the reaction of the starting materials and further growth of the particles seems to be inhibited by the formation of a protective PAA shell coordinating to the Cu(ɪɪ) ions.[30] At increasing amounts of PAA (and, hence, increasing acidity
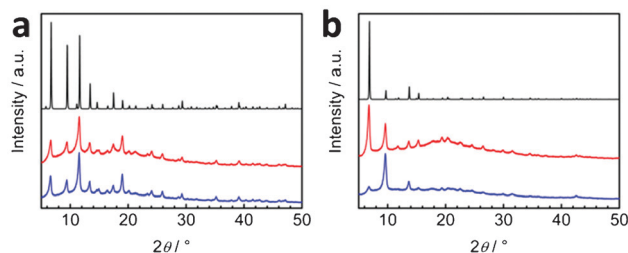

Fig. 1 PXRD patterns of HKUST-1 and IRMOF-3 nanoparticles. (a) Simulated XRD pattern for HKUST-1 (black) and PXRD patterns of HKUST-1 synthesized at 0 °C (red) and at RT (blue), (b) simulated XRD pattern for IRMOF-3 (black) and PXRD patterns of as-synthesized IRMOF-3 (red) and after drying (blue).

of the reaction mixture) the network formation (*i.e.* nucleation) is slowed down owing to a comparatively low supply of the network constituting deprotonated linker BTC^{3-}, along with a low availability of free copper ions not coordinated to PAA.[31] On the contrary, at very low PAA concentrations, the amount of stabilizing agent is insufficient to slow down monomer addition; thus, size defocusing is observed for both particularly low and high amounts of PAA (for a given concentration of H_3BTC and copper acetate). A ratio of 1 : 3 (0.123 mmol PAA) turned out to be most suitable to obtain a narrow size distribution (PdI = 0.091) and a reasonably high product yield (65–70%). Using these synthesis conditions, we observed no significant change of the size of the particles by increasing the reaction time from 5 min to 30 min (see Fig. S5 and S6, ESI†), which we attribute to the rapid formation and protection of the particles upon mixing of the starting materials with PAA.[32]

Nanosized IRMOF-3 was obtained by mixing $Zn(OAc)_2 \cdot 2H_2O$, 2-aminoterephthalic acid, CTAB and polyvinylpyrrolidone (PVP) in DMF at RT, and the formation of IRMOF-3 NPs was confirmed by PXRD (a mean diameter of 27 nm was deduced through the Scherrer formula). The diffraction pattern of the as-synthesized material matches with the simulated pattern, whereas the completely dry product shows an intensity reversion of the peaks at 6.7° and 9.6° (Fig. 1b). Similar findings for such an intensity change have been rationalized by pore-filling effects caused by residual guest species from the synthesis solution.[33]

The nanoparticulate morphology of IRMOF-3 was confirmed by SEM (Fig. 2c); we deduce a mean diameter of 36 nm from the SEM images, whereas AFM measurements suggest particle sizes between 12 nm and 45 nm (see Fig. 2d and S7, ESI†). We successfully achieved size control of the particles by varying the concentration of the CTAB–PVP mixture at a constant weight ratio of 1 : 1 between 0.0135 mmol/0.00013 mmol and 0.054 mmol/0.0005 mmol. DLS measurements suggest that higher amounts of the additives reduce the mean particle radius from 80 nm to <30 nm (see Fig. S8, ESI†). The combination of two differently acting stabilizers shows a synergetic effect on the size distribution of IRMOF-3 particles: while the use of either CTAB or PVP as size-controlling agent has shown to reduce the hydrodynamic radius of IRMOF-3 to around 40 nm with a broad size distribution in particular for PVP (n_{CTAB} = 0.027 mmol, and n_{PVP} = 0.00025 mmol, respectively; see Fig. S9, ESI†), the combination of both materials allows for the synthesis of even smaller particles (≈30 nm in radius for 0.027 mmol/0.00025 mmol of CTAB–PVP). To our knowledge, these sizes are among the smallest which have been reported so far for IRMOF-3 NPs and most other MOFs.[26–28] In order to investigate the effect of the additive combination on the particle size of IRMOF-3 in more detail, we conducted purely PVP-mediated syntheses as well as a direct mixing approach without the addition of any auxiliary material. DLS measurements suggest that increasing concentrations of PVP lead to a decrease of the particle radius from 280 nm down to 40 nm for the highest PVP concentration (0.00125 mmol)

(Fig. S10, ESI†). This observation is in agreement with a report about PVP protected Prussian Blue particles where an increased content of stabilizing PVP at given concentrations of the starting materials led to smaller diameters.[34] Besides size-modulating effects, PVP may prevent the particles from aggregating in solution.[35] The role of CTAB in the additive-mediated synthesis of IRMOF-3 may become clear by looking at the synthesis without mediators: in addition to small particles in the size range below 50 nm, SEM images reveal the presence of larger particles (80–180 nm) exhibiting a cubic morphology, which we did not observe in the presence of additives (Fig. S11, ESI†). According to previously described synthetic routes developed for the size- and shape-control of MOF NPs, CTAB has been shown to slow down the nucleation and growth of MOFs and, hence, to affect the resulting size distribution.[24,36,37] Here, it seems likely that the addition of CTAB in combination with PVP does not only restrict particle growth (for a given concentration of the additives), but also contributes to an increased uniformity in size. Interestingly, additional time-dependent experiments suggest that further increase of the reaction time from 5 min to 60 min in the presence of the additive mixture has little impact on the particle size and crystallinity of the final product (Fig. S12 and S13, ESI†). In contrast to the reaction of the pure starting materials (Zn source and H_2BDC–NH_2), which instantaneously causes turbidity of the reaction solution due to particle formation, the reaction speed for the additive-controlled synthesis of IRMOF-3 is slowed down dramatically such that (visible) crystal formation is delayed for a few minutes after combining the starting materials, which emphasizes the importance of CTAB and PVP as stabilizers (see Fig. S14, ESI†). Even after 11 days, the size distribution within the reaction mixture has changed only marginally from 30 nm (mean radius) to 48 nm (see Fig. S12, ESI†), suggesting a facile handling of the product and, moreover, the possibility to isolate a particular particle size within a narrow size range as a function of time.

MOF NPs with a uniform size of smaller than ≈100 nm can be used to build up optically homogeneous thin films exhibiting minimum scattering of visible light, which can serve as building blocks in MOF-based optical sensors.[38] MOF NP-based thin films may be deposited on a suitable substrate by solution processing, for example by spin- or dip-coating. As the layer thickness is affected by the concentration of particles in solution as well as by the volatility and wetting properties of the solvent, the use of well-dispersed MOF particles in an appropriate solvent is mandatory. Stable colloidal suspensions of HKUST-1 and IRMOF-3 were obtained by redispersing the particles in DMF, whereas their dispersion in other more volatile solvents such as ethanol or methanol was found to be impeded by the sedimentation of the particles within minutes. Thin films composed of HKUST-1 or IRMOF-3 particles were obtained by spin-coating DMF-based suspensions (conditions see ESI†) and characterized by cross-sectional SEM and ellipsometry. Fig. 3 shows a representative section of the MOF layers which exhibit uniform thicknesses (173 nm ± 15 nm for HKUST-1, 147 nm ± 5 nm for IRMOF-3) over a large
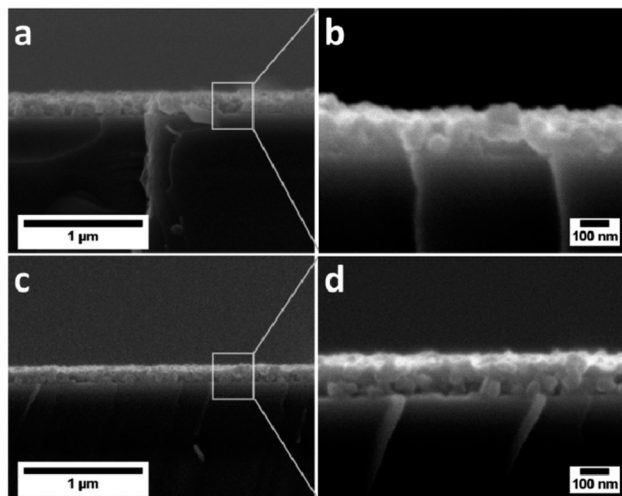
Fig. 3 Cross-sectional SEM images of MOF thin films assembled from colloidal solutions of the respective MOFs by spin-coating. (a) HKUST-1 film, (b) magnified detail, (c) IRMOF-3 film, (d) magnified detail.

lateral range; this thickness range is supported by ellipsometry (176.2 nm ± 0.6 nm for HKUST-1, 143.1 nm ± 0.2 nm for IRMOF-3). Besides layer thicknesses, ellipsometry allows us to determine the effective refractive index (RI) of a dielectric material (or composite) fashioned into a reflective thin film. We obtained effective RIs of 1.21 and 1.27 for HKUST-1 and IRMOF-3, respectively (note that textural porosity as well as possible residues of the respective additives contribute to the experimental value), which is slightly smaller than the RI of other MOF films (e.g. ZIF-8: 1.34–1.39).[38,39] The film assembly based on NPs imparts the MOF layer with textural porosity, which may be beneficial for MOF-based sensing devices: interstitial voids guarantee free diffusion throughout the entire film, thereby enhancing the sensitivity, whereas the MOF adds chemical selectivity to the system.[32,38]

Conclusions

In summary, we have developed a fast solvothermal synthesis approach toward sub-60 nm sized MOF NPs (HKUST-1 and IRMOF-3) under mild conditions. Our method allows fine-tuning of the particle size within a large range (30–300 nm) by adjusting the type and amount of polymer (PAA for HKUST-1) or polymer–surfactant combination (PVP–CTAB for IRMOF-3), along with the temperature and reaction time. The synergistic action of two different additives having characteristic stabilizing properties results in superior control of the IRMOF-3 particle size and monodispersity. Opening generally applicable synthetic avenues to MOF NPs with diameters smaller than commonly achieved size ranges (≈30 nm) is of importance for several fields of applications relying on ultrasmall MOF particles or thin films, such as in drug delivery or sensing. Along these lines, we have demonstrated the fabrication of optically homogenous HKUST-1 and IRMOF-3 thin films derived from stable colloidal MOF suspensions

by spin-coating. Such hierarchically porous structures bode well for the development of highly accessible and sensitive MOF-based sensing devices.

Acknowledgements

Notes and references

1 (a) M. Eddaoudi, D. B. Moler, H. Li, B. Chen, T. M. Reineke, M. O'Keefe and O. M. Yaghi, *Acc. Chem. Res.*, 2001, **34**, 319; (b) M. Eddaoudi, J. Kim, N. Rosi, D. Vodak, J. Wachter, M. O'Keefe and O. M. Yaghi, *Science*, 2002, **295**, 469; (c) C. Janiak and J. K. Vieth, *New J. Chem.*, 2010, **34**, 2366; (d) W. Xuan, C. Zhu, Y. Liu and Y. Cui, *Chem. Soc. Rev.*, 2012, **41**, 1677; (e) L. Song, J. Zhang, L. Sun, F. Xu, F. Li, H. Zhang, X. Si, C. Jiao, Z. Li, S. Liu, Y. Liu, H. Zhou, D. Sun, Y. Du, Z. Cao and Z. Gabelica, *Energy Environ. Sci.*, 2012, **5**, 7508; (f) S. M. Cohen, *Chem. Rev.*, 2012, **112**, 970; (g) T. R. Cook, Y. Zheng and P. J. Stang, *Chem. Rev.*, 2013, **113**, 734.

2 (a) M. P. Suh, H. J. Park, T. K. Prasad and D. Lim, *Chem. Rev.*, 2012, **112**, 782; (b) K. Sumida, D. L. Rogow, J. A. Mason, T. M. McDonald, E. D. Bloch, Z. R. Herm, T. Bae and J. R. Long, *Chem. Rev.*, 2012, **112**, 724.

3 (a) J. Lee, O. K. Farha, J. Roberts, K. A. Scheidt, S. T. Nguyen and J. T. Hupp, *Chem. Soc. Rev.*, 2009, **38**, 1450; (b) M. Ranocchiari and J. A. van Bokhoven, *Phys. Chem. Chem. Phys.*, 2011, **13**, 6388; (c) P. Valvekens, F. Vermoortele and D. De Vos, *Catal. Sci. Technol.*, 2013, **3**, 1435.

4 (a) J. Li, J. Sculley and H. Zhou, *Chem. Rev.*, 2012, **112**, 869; (b) M. Shah, M. C. McCarthy, S. Sachdeva, A. K. Lee and H. Jeong, *Ind. Eng. Chem. Res.*, 2012, **51**, 2179.

5 (a) B. Chen, S. Xiang and G. Qian, *Acc. Chem. Res.*, 2010, **43**, 1115; (b) L. E. Kreno, K. Leong, O. K. Farha, M. Allendorf, R. P. Van Duyne and J. T. Hupp, *Chem. Rev.*, 2012, **112**, 1105; (c) Y. Cui, Y. Yue, G. Qian and B. Chen, *Chem. Rev.*, 2012, **112**, 1126.

6 (a) O. Shekhah, J. Liu, R. A. Fischer and C. Wöll, *Chem. Soc. Rev.*, 2011, **40**, 1081; (b) D. Bradshaw, A. Garai and J. Huo, *Chem. Soc. Rev.*, 2012, **41**, 2344.

7 (a) P. Horcajada, C. Serre, D. Grosso, C. Boissière, S. Perruchas, C. Sanchez and G. Férey, *Adv. Mater.*, 2009, **21**, 1931; (b) A. Demessence, P. Horcajada, C. Serre, C. Boissière, D. Grosso, C. Sanchez and G. Férey, *Chem. Commun.*, 2009, 7149; (c) A. Demessence, C. Boissière, D. Grosso, P. Horcajada, C. Serre, G. Férey, G. J. A. A. Soler-Illia and

C. Sanchez, *J. Mater. Chem.*, 2010, **20**, 7676; (*d*) D. Jiang, A. D. Burrows, Y. Xiong and K. J. Edler, *J. Mater. Chem. A*, 2013, **1**, 5497.

8 (*a*) M. P. Attfield and P. Cubillas, *Dalton Trans.*, 2012, **41**, 3869; (*b*) N. Stock and S. Biswas, *Chem. Rev.*, 2012, **112**, 933; (*c*) E. A. Flügel, A. Ranft, F. Haase and B. V. Lotsch, *J. Mater. Chem.*, 2012, **22**, 10119; (*d*) V. Valtchev and L. Tosheva, *Chem. Rev.*, 2013, DOI: 10.1021/cr300439k.

9 (*a*) S. S. Y. Chui, S. M. F. Lo, J. P. H. Charmant, A. G. Orpen and I. D. Williams, *Science*, 1999, **283**, 1148; (*b*) P. M. Schoenecker, C. G. Carson, H. Jasuja, C. J. J. Flemming and K. S. Walton, *Ind. Eng. Chem. Res.*, 2012, **51**, 6513.

10 Q. Yang and C. Zhong, *J. Phys. Chem. B*, 2006, **110**, 655.

11 (*a*) Z. Li, L. Qiu, T. Xu, Y. Wu, W. Wang, Z. Wu and X. Jiang, *Mater. Lett.*, 2009, **63**, 78; (*b*) N. A. Khan and S. H. Jhung, *Bull. Korean Chem. Soc.*, 2009, **30**, 2921; (*c*) Z. Ni and R. I. Masel, *J. Am. Chem. Soc.*, 2006, **128**, 12394; (*d*) Z. Xiang, D. Cao, X. Shao, W. Wang, J. Zhang and W. Wu, *Chem. Eng. Sci.*, 2010, **65**, 3140; (*e*) N. A. Khan, E. Haque and S. H. Jhung, *Phys. Chem. Chem. Phys.*, 2010, **12**, 2625.

12 S. Loera-Serna, M. A. Oliver-Tolentino, Ma. de Lourdes López-Núñez, A. Santana-Cruz, A. Guzmán-Vargas, R. Cabrera-Sierra, H. I. Beltrán and J. Flores, *J. Alloys Compd.*, 2012, **540**, 113.

13 S. Diring, S. Furukawa, Y. Takashima, T. Tsuruoka and S. Kitagawa, *Chem. Mater.*, 2010, **22**, 4531.

14 (*a*) M. Schlesinger, S. Schulze, M. Hietschold and M. Mehring, *Microporous Mesoporous Mater.*, 2010, **132**, 121; (*b*) J. Klinowski, F. A. Almeida Paz, P. Silva and J. Rocha, *Dalton Trans.*, 2011, **40**, 321.

15 J. Zhuang, D. Ceglarek, S. Pethuraj and A. Terfort, *Adv. Funct. Mater.*, 2011, **21**, 1442.

16 G. Majano and J. Pérez-Ramírez, *Helv. Chim. Acta*, 2012, **95**, 2278.

17 L. Brinda, K. S. Rajan and J. B. B. Rayappan, *J. Appl. Sci.*, 2012, **12**, 1778.

18 H. Yang, S. Orefuwa and A. Goudy, *Microporous Mesoporous Mater.*, 2011, **143**, 37.

19 L. H. Wee, M. R. Lohe, N. Janssens, S. Kaskel and J. A. Martens, *J. Mater. Chem.*, 2012, **22**, 13742.

20 M. Gimeno-Fabra, A. S. Munn, L. A. Stevens, T. C. Drage, D. M. Grant, R. J. Kashtiban, J. Sloan, E. Lester and R. I. Walton, *Chem. Commun.*, 2012, **48**, 10642.

21 (*a*) S. Hermes, T. Witte, T. Hikov, D. Zacher, S. Bahnmüller, G. Langstein, K. Huber and R. A. Fischer, *J. Am. Chem. Soc.*, 2007, **129**, 5324; (*b*) J. Cravillon, R. Nayuk, S. Springer, A. Feldhoff, K. Huber and M. Wiebcke, *Chem. Mater.*, 2011, **23**, 2130; (*c*) M. Pham, G. Vuong, F. Fontaine and T. Do, *Cryst. Growth Des.*, 2012, **12**, 3091.

22 F. Wang, H. Guo, Y. Chai, Y. Li and C. Liu, *Microporous Mesoporous Mater.*, 2013, **173**, 181.

23 K. M. L. Taylor, A. Jin and W. Lin, *Angew. Chem.*, 2008, **120**, 7836.

24 Q. Liu, L. Jin and W. Sun, *Chem. Commun.*, 2012, **48**, 8814.

25 D. Jiang, T. Mallat, F. Krumeich and A. Baiker, *Catal. Commun.*, 2011, **12**, 602.

26 M. Ma, D. Zacher, X. Zhang, R. A. Fischer and N. Metzler-Nolte, *Cryst. Growth Des.*, 2011, **11**, 185.

27 L. Huang, H. Wang, J. Chen, Z. Wang, J. Sun, D. Zhao and Y. Yan, *Microporous Mesoporous Mater.*, 2003, **58**, 105.

28 Z. Gu, J. Jiang and X. Yan, *Anal. Chem.*, 2011, **83**, 5093.

29 J. Cravillon, S. Münzer, S. Lohmeier, A. Feldhoff, K. Huber and M. Wiebcke, *Chem. Mater.*, 2009, **21**, 1410.

30 Y. Gotoh, R. Igarashi, Y. Ohkoshi, M. Nagura, K. Akamatsu and S. Deki, *J. Mater. Chem.*, 2000, **10**, 2548.

31 T. Uemura, Y. Hoshino, S. Kitagawa, K. Yoshida and S. Isoda, *Chem. Mater.*, 2006, **18**, 992.

32 D. Tanaka, A. Henke, K. Albrecht, M. Moeller, K. Nakagawa, S. Kitagawa and J. Groll, *Nat. Chem.*, 2010, **2**, 410.

33 (*a*) J. Hafizovic, M. Bjorgen, U. Olsbye, P. D. C. Dietzel, S. Bordiga, C. Prestipino, C. Lamberti and K. P. Lillerud, *J. Am. Chem. Soc.*, 2007, **129**, 3612; (*b*) L. Zhang and Y. H. Hu, *Appl. Surf. Sci.*, 2011, **257**, 3392.

34 (*a*) T. Uemura and S. Kitagawa, *J. Am. Chem. Soc.*, 2003, **125**, 7814; (*b*) T. Uemura, M. Ohba and S. Kitagawa, *Inorg. Chem.*, 2004, **43**, 7339.

35 Z. Li and Y. Zhang, *Angew. Chem., Int. Ed.*, 2006, **45**, 7732.

36 P. Sarawade, H. Tan and V. Polshettiwar, *ACS Sustainable Chem. Eng.*, 2013, **1**, 66.

37 Y. Pan, D. Heryadi, F. Zhou, L. Zhao, G. Lestari, H. Su and Z. Lai, *CrystEngComm*, 2011, **13**, 6937.

38 (*a*) G. Lu and J. T. Hupp, *J. Am. Chem. Soc.*, 2010, **132**, 7832; (*b*) F. M. Hinterholzinger, A. Ranft, J. M. Feckl, B. Rühle, T. Bein and B. V. Lotsch, *J. Mater. Chem.*, 2012, **22**, 10356.

39 S. Eslava, L. Zhang, S. Esconjauregui, J. Yang, K. Vanstreels, M. R. Baklanov and E. Saiz, *Chem. Mater.*, 2013, **25**, 27.